Separation Science and Technology
Publication details, including instructions for authors and subscription information:
http://www.informaworld.com/smpp/title~content=t713708471

Pore Size Distributions of Polysulfonic UF Membranes and Protein Adsorption

P. Prádanos[a]; A. Hernández[a]
[a] DPTO. DE TERMODINÁMICA Y FÍSICA APLICADA FACULTAD DE CIENCIAS, UNIVERSIDAD DE VALLADOLID, VALLADOLID, SPAIN

To cite this Article Prádanos, P. and Hernández, A.(1996) 'Pore Size Distributions of Polysulfonic UF Membranes and Protein Adsorption', Separation Science and Technology, 31: 17, 2419 — 2441
To link to this Article: DOI: 10.1080/01496399608001057
URL: http://dx.doi.org/10.1080/01496399608001057

SEPARATION SCIENCE AND TECHNOLOGY, **31**(17), pp. 2419–2441, 1996

Pore Size Distributions of Polysulfonic UF Membranes and Protein Adsorption

P. PRÁDANOS and A. HERNÁNDEZ*
DPTO. DE TERMODINÁMICA Y FÍSICA APLICADA
FACULTAD DE CIENCIAS
UNIVERSIDAD DE VALLADOLID
E-47071 VALLADOLID, SPAIN

ABSTRACT

To compare actual and effective porous structure in operative conditions of ultrafiltration membranes, flux, retention, and the amount of adsorbed protein have been measured for 0.1% w/w aqueous solutions of several proteins [lysozyme, pepsin, bovine serum albumin (BSA), lipase, and γ-globulin] with molecular weights from 14.6 to 150 kD tangentially filtered through two asymmetric polysulfone membranes, E-100 and E-500. From retention and flux experiments, the dependency of mass transfer coefficients on molecular volume has been analyzed. Results imply that protein molecules behave as being slightly uncoiled, especially when filtered through the smallest pore size membrane. By using a simple sieving model, retention data allow pore size distributions to be obtained. The data are modified by taking into account adsorption and volume hindrance effects in operational conditions.

Key Words. Crossflow ultrafiltration; Polysulfonic membranes; Protein diffusivities; Adsorption; Pore size distributions

INTRODUCTION

Ultrafiltration (UF), a pressure-driven separation process capable of gently retaining species in the molecular weight range of 300 to 500,000, is

* To whom correspondence should be addressed. E-mail: membrana@wamba.cpd.uva.es

being substituted for some more traditional concentration and separation processes in a variety of industries. In the early 1980s more than 34 UF applications were in use. These included applications in the food industry, pharmaceuticals and biotechnology, and water purification and waste treatment in the chemical and paper industries (1–3). Protein filtration has a relevant role in most of these industries: in dairy processes, in wine stabilizing, in fruit juice clarification, in the recovery of valuable macromolecules from fermentation broths, in the paper and pulp industry, and in the continuous production and separation of biomolecules in enzymatic processes, among others.

Most of these applications use polysulfone membranes either in spiral wound, tubular, or hollow fiber modules. These membranes have especially desirable characteristics due to their molecular structure where units of diphenylene sulphone are repeated, as pointed out by Gekas et al. (4). The SO_2 group in the polymeric sulfone is quite stable due to the electronic attraction of resonating electrons between adjacent aromatic groups. The oxygen molecules projecting from this group each have two pairs of unshared electrons to donate to strong hydrogen bonding of solute or solvent molecules. This makes polysulfone membranes very resistant with a pH range of 1 to 14, quite good chlorine resistance, and a wide temperature range with hydrophobic properties if untreated.

There are some drawbacks with ultrafiltration as well. Given that once a membrane retains a molecule or particle, it should also permit high solvent fluxes in order to obtain a high efficiency of the ultrafiltration step. However, it is known that permeability decreases until it becomes more or less constant for high pressures. The existence of such a maximum for the flux has been attributed to concentration-polarization; i.e., the accumulation of the rejected solute in a boundary layer in contact with the membrane surface. In these conditions, the resulting mechanism of flux reduction can be attributed, according to Vilker et al. (5), to: 1) a reduction in the driving force due to the increase in osmotic pressure at the membrane surface, 2) gelation of the retained solute with the creation of an extra hydraulic resistance, or 3) a fouling process.

The previous work on protein adsorption is far too extensive to be resumed here, and the reader is referred to the review by Andrade (6) for a more detailed discussion. Nevertheless, there is considerable experimental evidence that protein adsorption within the pores of UF membranes can dramatically alter membrane transport properties. Reduction of membrane hydraulic permeability, increases in true retention coefficient, and hindered diffusivities are known (7–9). This suggests that protein adsorption reduces the effective membrane pore size and/or there is a process of pore blocking (fouling).

Fouling could be partly due to irreversible adsorption but also to other deposition phenomena mainly determined by sieving effects. In any case, it can be substantially reduced if the solute–surface interactions are minimized by decreasing the membrane–protein affinity or contact times. This can be done, for example, by using tangential filtration with a high enough speed over the retentate face. This would also sweep the membrane surface making entrapment of protein molecules on the pore entrances more difficult, which should reduce pore clogging. Another way to limit protein–surface interaction should be by controlling the pH level, as shown by Bowen and Gan (10).

It is known that solute transport through constricted pores is reduced compared to that in bulk solution due to two phenomena: 1) equilibrium partitioning, which reduces the solute concentration in the pores due to both steric effects and electrostatic interactions, and 2) hydrodynamic effects, which increase the frictional drag on the solute molecules. Both effects should lead to a retention coefficient for molecules and pores of constant sizes that should be calculated in terms of λ (11), which is defined as the ratio between the mean projected solute diameter and the specific area of the pores (pore volume/pore surface area). Several possibilities for such a relationship have been suggested for different ranges of the Peclet number and pore and molecule shapes (12–17). Nevertheless, the situation is extremely complicated if pore as well as solute size distributions have to be considered. In connection with this problem, many authors have attempted to relate pore or molecular size distributions (separately) to retention data (18–21), all them concluding that it is impossible to arrive at significant relations unless a known shape is assumed for the distribution being considered.

The manufacturers of membranes for ultrafiltration usually give only the nominal molecular weight cut-off for their products. However, in actual application there is not a sharp edge between the molecular weights of solutes passing freely through the membrane and those retained, especially if the membrane heteroporosity and/or solute polydispersity are taken into account. On the other hand, for concentration-polarization the molecular weight cut-off depends on the pressure difference acting through the membrane and the velocity of retentate recirculation in tangential ultrafiltration. Consequently, the corresponding retention characteristics should be studied in detail for each membrane and application in order to obtain the structural characteristics in operative conditions.

Our aim here is to study the pore size distributions of two polysulfone membranes as determined by the tangential ultrafiltration of proteins, whose solutions will be considered as monodisperse. This will be done without assuming an "a-priori" shape for the pore size distribution, thus

no volume hindrance leading to effective pore size distributions affected by both adsorption and friction inside the pores will be explicitly considered. In this way, these distributions are operative bounded, and that should help in selecting the correct membrane to retain a given protein of a known free solution size.

A secondary objective is to examine how the structure of protein molecules is modified through an analysis of the dependence of pore entrance diffusivities on molecular volume. Measured irreversible adsorption will be compared with other factors causing flow difficulties (retaining adsorption in operative conditions along with friction and partition equilibrium) in filtration, and how both groups of phenomena depend on pore size. The operative pore size distributions will be contrasted with those obtained by subtracting the adsorption layers.

Two commercially available asymmetric polysulfone membranes, E-100 and E-500 (made by Desalination Systems Inc.), have been selected. Their nominal mean diameters are 10 and 40 nm, respectively. A neutral pH is used in order to reproduce the most common conditions in natural media and bioreactors. Moreover, E-100 and E-500 seem to be almost discharged at neutral pH, which should reduce adsorption. On the other hand, if the proteins selected have a relatively strong negative charge at neutral pH, this should prevent the formation of protein aggregates. This is the case with the proteins we have selected: lysozyme, pepsin, bovine serum albumin (BSA), lipase, and γ-globulin. They cover molecular weights from 10,000 to 15,000 daltons and can be assumed as substantially nonpolydispersed molecules.

MATERIALS AND METHODS

Chemicals

Two flat asymmetric polysulfone membranes obtained by phase inversion were used. They are commercialized under the names E-100 and E-500 as ultrafiltration spiral modules (Desalination Systems Inc.). Several characteristics of these spiral module membranes as provided by the manufacturer are shown in Table 1.

In order to avoid any irreversible change during operation, each membrane sample was pressurized at 1000 kPa for 2 hours before being used (no permeability change could be detected for longer pressurizing periods). Aqueous solutions of several proteins (lysozyme, pepsin, bovine serum albumin, lipase, and γ-globulin) with molecular weights of 14,600, 36,000, 67,000, 80,000 and 150,000 daltons, respectively, were used (lysozyme was not used with E-500 because no retention was observed). All the proteins were obtained from Fluka AG: lysozyme (EC 3.2.1.17), lyophi-

TABLE 1
Operating and Design Parameters for E-100 and E-500 Ultrafiltration Spiral Elements

Membrane	Pore size (μm)	M_w cut-off[a]	$L_{p,n}$ (m/s·Pa)[b]	Maximum pressure (Pa)	Maximum temperature (K)	pH	Chlorine tolerance (ppm/day)
E-100	0.01	35,000	7.12×10^{-11}	41×10^5	323	2–11	5000
E-500	0.04	500,000	2.70×10^{-10}	41×10^5	323	2–11	5000

[a] Test conditions: Aqueous solutions of 1% dextran to 50,000 Pa and 298 K.
[b] Specifications are based on fouling free water at 200,000 Pa, 298 K, and 8.25 m^2 active area.

lized, dialyzed, and salt-free from hen egg white of >95% purity; pepsin (EC 3.4.23.1), crystalline powder from hog stomach; BSA of >98% purity; lipase (EC 3.1.1.3), fine powder from *Rhizopus arrhizus*; and γ-globulin from bovine blood of >98% purity.

The aqueous solution used was a relatively dilute 0.1% w/w in order to minimize solute–solute interactions. It was prepared with distilled, degassed, and deionized water (resistivity higher than 18 MΩ·cm), and all solutions were previously prefiltered with a microfiltration inorganic membrane (Anopore filter A02, whose nominal pore diameter is 0.2 μm) in order to eliminate large residual particles. All concentrations were measured by using the Lowry assay (22) with a spectrophotometer set at 750 nm.

A pH buffer ($HNa_2PO_4 \cdot H_2NaPO_4$ at 8.1×10^{-3} and 1.9×10^{-3} N) of 7.4 was used along with a bactericidal agent (NaN_3) at 0.02% w/w, giving an ionic strength of $I = 0.021$ N. According to Kirkwood (23) and Malamud and Drysdale (24), the isoelectric points are 11 for lysozyme, between 2.2 to 2.8 for pepsin, from 4.7 to 4.9 for BSA, 4.0 for lipase, and from 6.1 to 6.47 for γ-globulin. Therefore, all the proteins used are negatively charged at neutral pH. This and the presence of added salts as buffers and bactericides, which increase the ionic strength, prevent the formation of aggregates.

Finally, a solution of 50 g/L sodium dodecyl sulfate (SDS) in 0.5 N NaOH was used to desorb the protein. All reagents were of analytical grade and obtained from Fluka.

Experimental Setup

All the experiments were performed in isothermal conditions at 298 K by using a flat membrane tangential ultrafiltration device that has been described elsewhere by us (25). The membrane cell is a Minitan-S manifold from Millipore made of methacrylate. On the membrane there are nine

ducts of rectangular section 0.40 × 7.0 mm and a length (L) of 55.0 mm. The resulting channel hydraulic diameter (d_h) is 0.76 × 10^{-3} m, giving an effective membrane area of 3.68 × 10^{-3} m^{-2} and a channel section of 2.8 × 10^{-6} m^{-2}.

The solution is extracted from a thermostated reservoir by means of a regulatable impulsion pump. Two pressure transducers are placed before and after the membrane holder in the retentate loop. They have a range of 0 to 1000 kPa over the atmospheric pressure, with an accuracy of ±0.25% full scale. Given that the pressure loss along the hydraulic channel of the permeate loop is small and may be assumed as almost linear, the transmembrane pressure can be taken as the average of the values taken up and down the membrane cell. The applied transmembrane pressures were below 1000 kPa in all cases.

In order to measure the retentate flow, two electromagnetic flowmeters are used, whose ranges are 1 × 10^{-6} to 1 × 10^{-5} m^3/s and 1.67 × 10^{-5} to 1.67 × 10^{-4} m^3/s, both with errors lower than ±0.25% full scale. The speed and pressure in the retentate loop are independently controlled by means of the pump regulation and an appropriate needle valve. The resulting recirculation speeds used have been 0.040 ± 0.001, 0.066 ± 0.001, 0.132 ± 0.001, 0.198 ± 0.001, 0.264 ± 0.002, 0.330 ± 0.002, 0.396 ± 0.006, 0.660 ± 0.019, 0.99 ± 0.02, and 1.980 ± 0.03 m/s. These speeds are defined as the volume flow through the hydraulic channel per unit time and unit cross-sectional area, hence they are averaged for a channel section.

The volume flux of permeate through the membrane is measured by timing and weighting with a high precision balance with errors lower than ±1 × 10^{-7} kg. The retentate and permeate concentration are measured by the already mentioned spectrophotometric method.

In order to characterize clean and fouled membranes, the water permeability (hydrodynamic permeability) is measured prior to any contact with protein solutions and also for used membranes. The fouled membranes are water washed under pressure (1 MPa) for 1 hour in the same experimental device. To remove adsorbed protein from the used membranes, they are immersed for 3 hours at 303 K in the SDS solution. Afterward, the protein concentration of this solution is measured as mentioned.

THEORETICAL ASPECTS

To follow the outlined pattern, we will start by providing the necessary theoretical background to obtain mass transfer coefficients and study their dependency on molecular volume as well as the method to estimate pore size distributions from them.

Mass Transfer Coefficients and Diffusivities

The true retention coefficient can be defined as $R = 1 - c_p/c_m$, which relates the actual concentrations on both faces of the membrane: c_m-retentate concentration in contact with the membrane (bigger than the feed concentration c_0 due to concentration-polarization) and c_p = permeate concentration. Nevertheless what is directly accessible is the observed retention coefficient, $R_o = 1 - c_p/c_0$.

The mass transfer coefficient, which is sometimes defined as the ratio between the diffusion coefficient in the concentration-polarization layer and its thickness, $K_m = D/\delta$, can be calculated on the basis of heat transfer analogies according to the Graetz-Lévêque correlation as shown, for example, by Hwang and Kammermeyer (26):

$$K_m = A\left(\frac{D^2}{d_h L}\right)^{1/3} v^\alpha = \Phi v^\alpha \tag{1}$$

where A and α are constants.

Thus, in terms of the so-called film model, Φ can be evaluated according to

$$\ln\frac{1 - R_o}{R_o} = \ln\frac{1 - R}{R} + \frac{J_V}{\Phi v^\alpha} \tag{2}$$

by a plot of $\ln[(1 - R_o)/R_o]$ against J_V/V^α, in conditions of pressure-independent flux, that should be a straight with $1/\Phi$ as the slope and an ordinate intercept of $\ln[(1 - R)/R]$.

Several values have been proposed for the coefficients A, α. According to Cheryan (2) and Van den Berg et al. (27), this exponent seems to depend on the flow regime in such a way that values of α = 1/3 or 1/2 can be used for the laminar regime that we will use here (Reynolds numbers from 34 to 1670).

According to Eq. (1), Φ is proportional to $D^{2/3}$. In order to study the actual behavior of protein molecules entering the pores during filtering, it will be useful to analyze the dependency of the measured Φ on the molecular volume obtained from the protein gyration radii, which can be compared with those predicted by different theories on molecular behavior.

According to the Einstein equation:

$$D = kT/f \tag{3}$$

where k is the Boltzmann constant, T is the temperature, and f is the molecular friction coefficient. If the protein molecules are assumed to be nondraining (solvent molecules within the coiled polymer chain moving

with it) and represented by an equivalent impermeable hydrodynamic sphere of radius r, then, according to Stokes' law:

$$f = 6\pi\eta r \tag{4}$$

Nevertheless, by making the reasonable assumption that r is proportional to $\langle s^2\rangle^{1/2}$ (i.e., the root-mean-square of distances of chain segments from the center of mass of the molecule or radius of gyration), Eq. (4) can be rewritten in the form

$$f = K_0\alpha_\eta\langle s^2\rangle_0^{1/2} \tag{5}$$

where K_0 is a constant for a given system, α_η is the expansion parameter for the hydrodynamic chain dimensions, and $\langle s^2\rangle_0^{1/2}$ is the radius of gyration of an unperturbed molecule (i.e., measured in conditions of no excluded volume). Then, according to the Kirkwood–Riseman theory:

$$K_0\alpha_\eta = \frac{3}{8}(6\pi^3)^{(1/2)}\eta \tag{6}$$

But, for real polymer molecules, as pointed out by Young and Lovell (28), $\langle s^2\rangle_0^{1/2}$ is proportional to $x^{1/2}$, where x is the number of segments of the molecule. For highly expanded coils, α_η is approximately proportional to $x^{1/10}$. Thus, by also taking into account that the number of segments should be proportional to the molecular weight M_w, Eqs. (3) and (5) lead to

$$D = K_0'/M_w^a \tag{7}$$

where K_0' is another constant and a should be approximately equal to 0.6 for large expansions and nondraining molecules.

On the other hand, for free-draining molecules, i.e., when solvent molecules are able to flow past each segment of the chain,

$$f = x\xi \tag{8}$$

where ξ is the frictional coefficient for each segment. This leads to

$$D = K_0'/M_w \tag{9}$$

Thus, in this case, $a = 1$ in Eq. (7). This leads to a values in the range from 0.6 to 1 depending on the draining or nondraining behavior of the protein molecules when moving through the membrane.

On the other hand, Young et al. (29) showed, from measurements of 301 proteins with molecular weights in the 13 to 370 kD range, that the partial specific volume of proteins is from 6.9 to 7.8 $\times$ 10^{-2} m^3/kg, a relatively narrow Gaussian distribution, with a mean value of 7.3 $\times$ 10^{-2} m^3/kg. Consequently, the partial specific volume can be considered as approximately constant for all proteins, thus leading to

$$V \propto M_w \tag{10}$$

i.e., the molecular volume V should be nearly proportional to the molecular weight. Thus, finally, Eqs. (1), (7), (9), and (10) lead to

$$\Phi = (K/V^a)^{2/3} \tag{11}$$

Pore Size Distribution

In order to evaluate the pore size distributions of a partially retaining membrane, it can be assumed, according to an original idea of Michaels (30) as developed by Le and Howell (31), that the retention is due to a sieving mechanism in such a way that for each molecular weight there is a fraction of totally retaining pores while the rest of them allow the molecules to pass. Hence, assuming no effect of friction and partition equilibrium in the pore entrances according to the approach that will be followed here, we can write the mass balance for each molecular weight as

$$J_V c_p = J_{V,t} c_m \tag{12}$$

where $J_{V,t}$ is the volume flux transmitted through the nonrejection fraction of pores. On the other hand, the ratio of the transmitted volume and water fluxes is, according to Darcy's law:

$$\frac{J_{V,t}}{J_{w,t}} = \frac{\eta(c_m)}{\eta(0)} \tag{13}$$

where $\eta(c_m)$ and $\eta(0)$ are the solution and solvent viscosities, respectively. But, for low c_m, (32), this ratio is approximated to 1 in such a way that Eq. (12) can be rewritten as

$$J_{w,t} = J_V(1 - R) \tag{14}$$

Therefore, $J_{w,t}$ can be evaluated once J_V for each R is known. Then, by using again the mass balance:

$$\left.\begin{aligned} J_V c_p &= J_s \\ J_V - J_s &= J_w \end{aligned}\right\} \tag{15}$$

which allows J_w to be obtained if c_p is also known. Consequently, $J_{w,t}/J_w$ can be calculated for each c_p and R; i.e., for each molecular weight or gyration radius of the five proteins as obtained from the literature (33–36). Thus, it gives the cumulative fraction of flux passing through all nonrejecting pores for each molecular size (which can be taken as equivalent to the corresponding pore sizes, d_p, if volume hindrance and adsorption contributions are not considered), while its derivative should provide the flux through pores of a given radius allowing proteins of this size to pass.

In order to increase accuracy in the numerical derivation process, an analytical function can be used to interpolate $J_{w,t}/J_w$ vs d_p. In order to reproduce well the experimental data, a logicial curve, with horizontal asymptotes at $J_{w,t}/J_w = 1$ and 0; i.e.,

$$\frac{J_{w,t}}{J_w} = \frac{1}{\left[1 + \left(\frac{d_p}{B}\right)^C\right]} \tag{16}$$

seems appropriate. B and C are constants to be evaluated by fitting Eq. (16) to the experimental results. In this way $d(J_{w,t}/J_w)/d(d_p)$ can be easily obtained and normalized.

Finally, the differential flux fraction can be correlated with the pore fraction according to the Hagen-Poiseuille equation in such a way that

$$f_d(N/N_T) \equiv \frac{d(N/N_T)}{d(d_p)} = \frac{d(J_{w,t}/J_w)}{d(d_p)} \frac{K_n}{d_p^4} \equiv f_d(J_{w,t}/J_w) \frac{K_n}{d_p^4} \tag{17}$$

K_n is a normalization constant.

RESULTS AND DISCUSSION

Mass Transfer Coefficients and Diffusivities

In order to evaluate the mass transfer coefficient as a function of v, we can plot Eq. (2) for several constant pressure differences and variable recirculation speeds. Of course, the pressures used should be high enough to be in the zone of J_v, almost independent of Δp as shown elsewhere by us (37). Then, we can obtain Φ directly for each protein and membrane [see Prádanos and Hernández (38) for details], leading to values of Φ with a 95% confidence level (t-tested).

The values of ϕ so obtained are presented in Fig. 1 as a function of the molecular volume of the protein, V, which is obtained from the gyration radii. If Eq. (11) is fitted to experimental data, the values of K and a are as shown in Table 2. It is seen that the values of a are well within the expected range.

Adsorption

The amount of adsorbed proteins can be measured as mentioned above. The total number of deposited molecules multiplied by the mean section of the molecule (evaluated by assuming spherical molecules of the gyration radii) gives the total area occupied by proteins if an adsorption monolayer is assumed. This conjecture should agree with a Langmuir-type adsorption as usually assumed [see, for example, Robertson and Zydney (39)] for

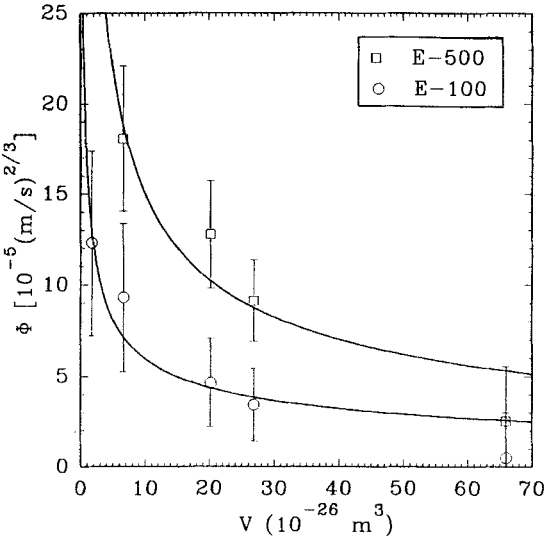

FIG. 1 Φ as a function of protein volume for both membranes. The solid lines refer to Eq. (11) with the constants shown in Table 2.

protein adsorption. The ratio between the occupied area and the cross-section area of the membrane, A_a/A_m, is shown as a function of $(\log M_w)^{-1}$ in Fig. 2.

It is seen that A_a/A_m is higher for E-100 than for E-500, which means that E-100 (the membrane with smaller pores) has a higher internal area, which is not surprising. On the other hand, the occupied membrane area is almost constant for low molecular weight proteins while it decreases steeply for increasing M_w (in fact for γ-globulin), indicating that adsorption is limited for nonpenetrating or scarcely penetrating proteins.

On the other hand, the protein adsorption can also be studied in terms of water permeabilities for new ($L_{p,n}$) and used ($L_{p,u}$) membranes, shown

TABLE 2
Fitted Parameters for Eq. (11)

	K (10^{-26} m^{3a+1}/s)	a (dimensionless)
E-100	973 ± 251	0.67 ± 0.16
E-500	0.36 ± 0.22	0.83 ± 0.25

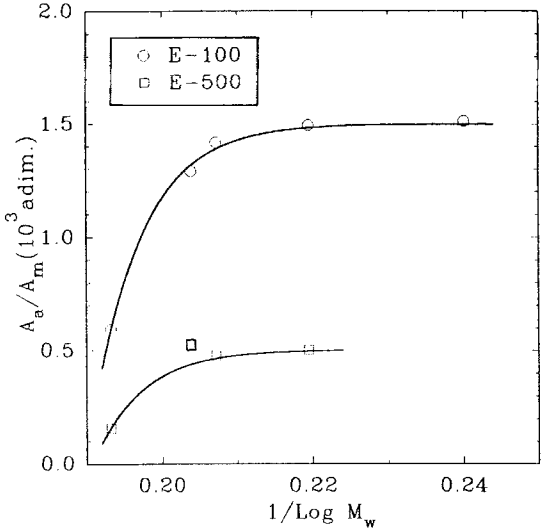

FIG. 2 Adsorbed surface per unit of membrane area as a function of the molecular weight.

in Fig. 3. It is seen that these permeabilities decrease with M_w faster for E-500 than for E-100, giving similar values for γ-globulin, while the results for low molecular weights approximate the new membrane permeability.

A coverage ratio can be defined in terms of the pore diameters for new (d_n) and used (d_u) membranes as

$$\theta = \frac{d_n - d_u}{2d} \tag{18}$$

where d is the equivalent diameter ($2r$) of the protein molecule. θ can be obtained once d_u is known [according to the Hagen-Poiseuille equation, it is $d_n(L_{p,u}/L_{p,n})^{1/4}$] and the nominal value is taken for d_n. The corresponding results are shown in Tables 3 and 4 and should correspond to the number of adsorption layers in the pores of membranes in use. It is seen that this coverage factor increases with M_w and is greater for E-500 than for E-100 because of the greater space for adsorption in larger pores than inside narrower ones.

Both A_a/A_m and θ are calculated from measures of fouled membranes that were previously washed with water under pressure (as already mentioned). Thus, possibly they refer to irreversible adsorption which should be lower than the real dynamic adsorption under operative conditions.

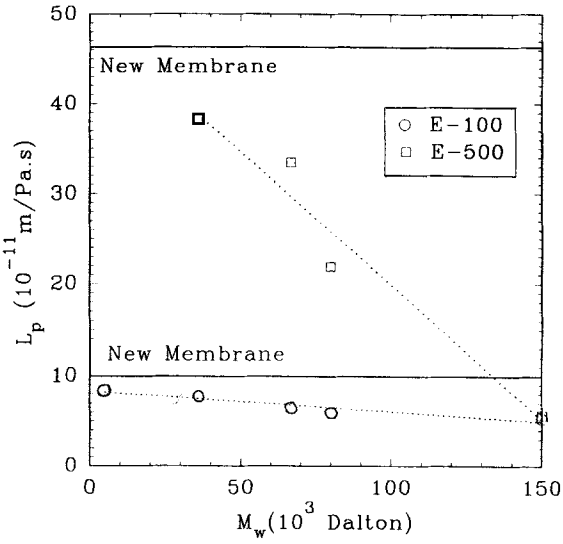

FIG. 3 Hydrodynamic permeabilities for new and used membranes as a function of molecular weight.

Pore Size Distributions

Once the mass transfer coefficients have been obtained, the concentration in contact with the membrane, c_m, and the true retention coefficient, R, can be calculated. It is seen that a retention close to a 100% (99.9% for E-100 and 97.0% for E-500) is obtained for γ-globulin, i.e., for an equivalent molecular diameter of 0.0108 μm for both membranes. In fact, this value should only be the maximum diameter in pore size distribution

TABLE 3
Water Permeability and the Pore Radius Obtained According to the Hagen–Poiseuille Equation for E100. For a New Membrane the Water Permeability, $L_{p,n}$, Is 9.94×10^{-11} m/Pa·s and the Nominal Diameter, d_n, Is 1×10^{-8} m

Fouled with	$L_{p,u}$ (10^{-11} m/Pa·s)	d_u (10^{-9} m)	θ
Lysozime	8.42	9.60	0.063
Lipase	7.74	9.40	0.060
BSA	6.46	8.98	0.071
Pepsin	5.91	8.78	0.076
γ-Globulin	5.31	8.54	0.067

TABLE 4
Water Permeability and the Pore Radius Obtained According to the Hagen–Poiseuille Equation for E500. For a New Membrane the Water Permeability, $L_{p,n}$, Is 46.31×10^{-11} m/Pa·s and the Nominal Diameter, d_n, Is 4×10^{-8} m

Fouled with	$L_{p,u}$ (10^{-11} m/Pa·s)	d_u (10^{-9} m)	θ
Lipase	38.35	38.16	0.184
BSA	33.46	36.88	0.217
Pepsin	21.90	33.18	0.426
γ-Globulin	5.66	23.66	0.756

if the protein molecules are assumed as rigid, without friction, and nonadsorbing.

According to the method outlined above, the pore size distributions can be obtained. In effect, $J_{w,t}/J_w$ can be evaluated according to Eqs. (14) and (15), nonlinearly fitted to Eq. (16), and represented versus gyration diameters that, as mentioned, can be assumed as equal to the corresponding pore sizes if neither volume hindrance neither adsorption are taken into account. This curve can then be numerically differentiated and normalized to give the differential flux distribution. Finally, the differential pore number distribution can be estimated by using Eq. (17) and normalizing to 1. The results so obtained are presented in Fig. 4 and 5.

These distributions are fitted to lognormal functions according to

$$f(x) = f_{max}(\mu) \exp\left\{ -\left[\frac{\log\left(\frac{x}{\mu}\right)}{\log \sigma} \right]^2 \right\} \tag{19}$$

where μ is the mean x and σ is its standard deviation. Here d_p plays the role of the x variable, leading to fitted means and standard deviations with confidence levels over 99.5%.

In this way, mean pore diameters of 6.06 ± 1.54 and 7.33 ± 1.32 nm have been obtained for the flux differential distributions with slightly smaller means and deviations for the pore number distributions. These results are far below the nominal data given in Table 1 and are quite similar for both membranes in spite of their very different nominal pore sizes.

On the other hand, these distributions can be modified if adsorption is taken into account. This can be done by an iterative procedure; i.e., increasing the dynamic coverage ratio θ_d, which should be equal for all the

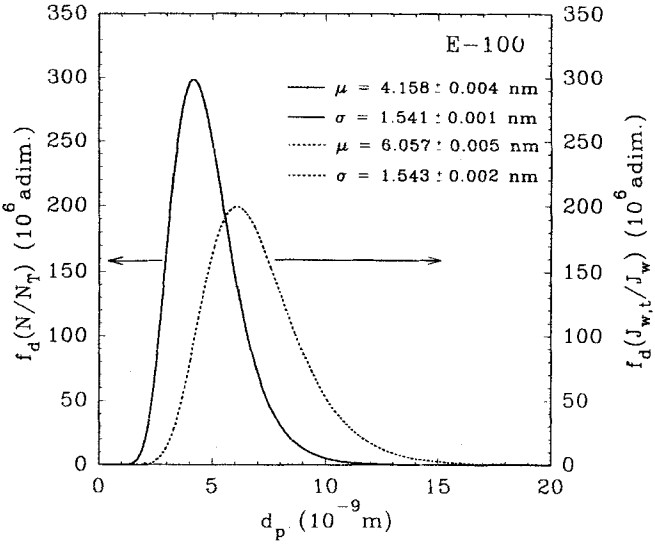

FIG. 4 Pore number and flux distribution functions versus pore diameters for E-100. μ is the average and σ the standard deviation.

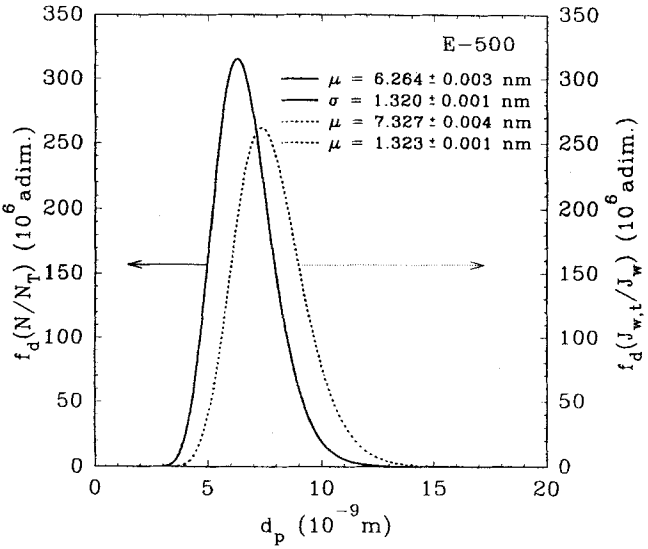

FIG. 5 Pore number and flux distribution functions versus pore diameters for E-500. μ is the average and σ the standard deviation.

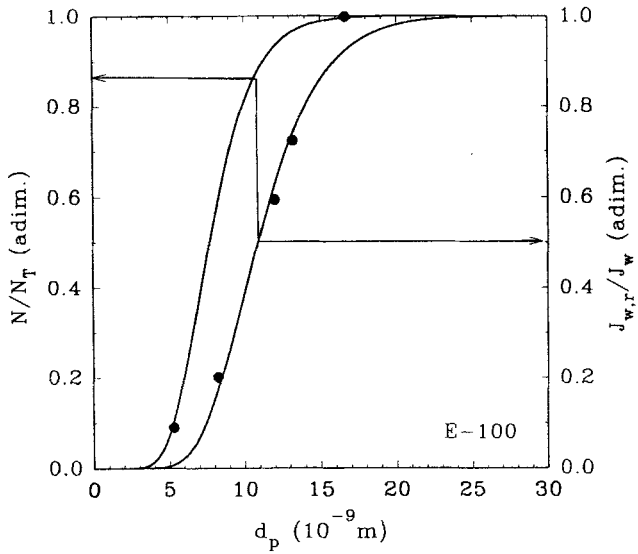

FIG. 6 Flux and pore number cumulative distribution functions versus pore diameters for E-100, assuming adsorption. Note that half the flux should pass through 15% of the wider pores. Here $J_{w,r}/J_w$ is $1 - (J_{w,t}/J_w)$.

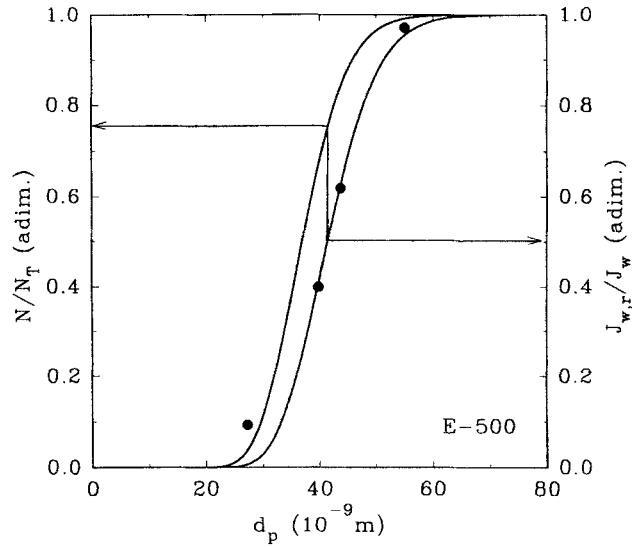

FIG. 7 Flux and pore number cumulative distribution functions versus pore diameters for E-500, assuming adsorption. Note that half the flux should pass through 25% of the wider pores. Here $J_{w,r}/J_w$ is $1 - (J_{w,t}/J_w)$.

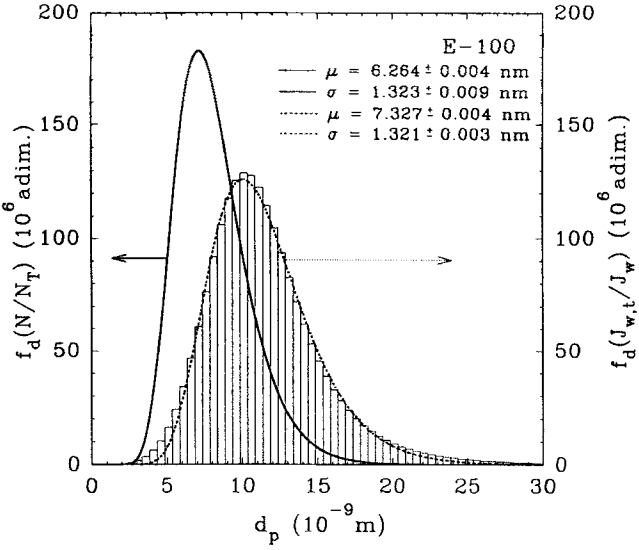

FIG. 8 Flux and pore number differential distribution functions versus pore diameters for E-100, assuming adsorption. μ is the average and σ the standard deviation.

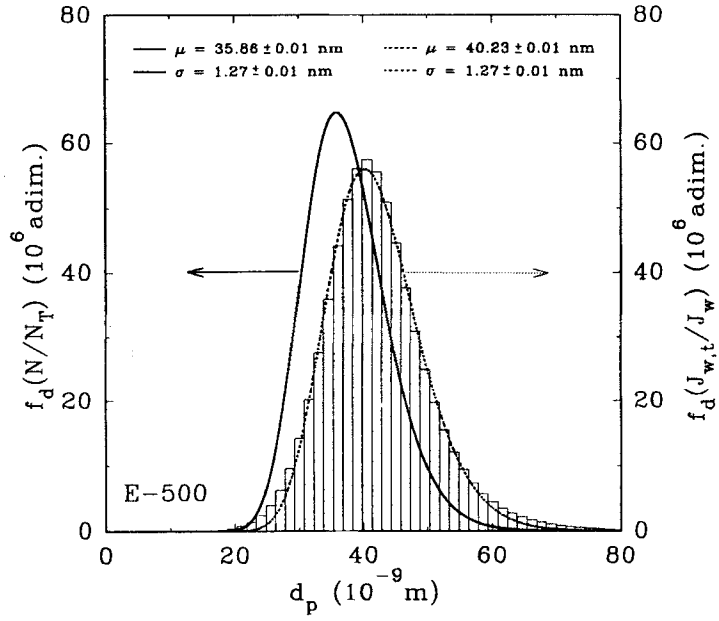

FIG. 9 Flux and pore number differential distribution functions versus pore diameters for E-500, assuming adsorption. μ is the average and σ the standard deviation.

proteins, thus being an average, until the flux distribution function gives a mean pore size equal to the nominal pore size. This distributions so obtained are shown in Figs. 6 to 9 and correspond to θ_d values of 0.326 and 2.230 for E-100 and E-500, respectively. It is seen that the results so obtained for pore sizes are $(10.04 \pm 1.52) \times 10^{-9}$ m for E-100 and $(40.23 \pm 1.27) \times 10^{-9}$ m for E-500 from the flux distributions, while for the pore number distributions the central representatives of the distributions are $(7.10 \pm 1.52) \times 10^{-9}$ m for E-100 and $(35.86 \pm 1.27) \times 10^{-9}$ m for E-500.

CONCLUSIONS

We have studied the structural characteristics in functional operative conditions of two ultrafiltration asymmetric membranes in crossflow ultrafiltration of proteins. In order to obtain pore size distributions, it was necessary to measure the apparent or observed coefficient of retention and correct it to obtain the real one. This has been done in accordance with the film model for the concentration-polarization phenomenon.

The mass transfer coefficient of the proteins is calculated by varying the recirculation velocity at constant pressure. A value of $\alpha = 1/3$ has been used in Eqs. (1) and (2); it is predicted by many different correlations for laminar flow and flat or tubular membranes [see, for example, the Graetz-Lévêque's or Sourirajan's relationships in Cheryan (2) and Hwang and Kammermeyer (26)]. On the other hand, this value for α has also been proved to fit the data better.

The mass transfer constant, Φ, should depend on the pore entrance diffusivities and ultimately on molecular volumes. This dependency has been studied within the frame of current macromolecular theories, leading to results which are compatible with molecular states of mean expansions and solvent penetration, but showing slightly larger extensions of molecular segments for the molecules of proteins permeating through the E-100 membrane than across E-500: values of the exponent a in Eq. (11) are 0.6 (nondraining) $<$ 0.67 (E-100) $<$ 0.83 (E-500) $<$ 1 (free draining). This should mean that protein molecules lose, to some certainly limited extent, their coiled structure, thus limiting solvent penetration in being forced to pass through narrower pores. It is worth noting that for less adsorptive membranes, where protein molecules should remain approximately spherical, Eqs. (3) and (4) should lead to a diffusion coefficient proportional to $V^{-1/3}$, as shown by us for inorganic membranes (37). This seems to correlate with a certain decoiling process with relevant adsorption levels.

Referring to irreversible adsorption, both A_a/A_m and θ have been evaluated by assuming that all pores are freely penetrated by the protein mole-

cules, which is evidently not totally true, at least for the biggest proteins, because a significant decrease of adsorption and water permeability should be due to blocking of a portion of pores. Due to these factors, A_a/A_m is underestimated while θ is overestimated. On the other hand, the occupied surface fraction is even more undervalued due to the existence of less than a complete layer of adsorbed protein (θ is always less than 1).

It is seen for real retentions that an equivalent molecular radius of 0.0108 μm (γ-globulin) corresponds to 100% retention for E-100 and 97% for E-500. This value is similar to the nominal pore size for E-100 while it is near to a fourth of the nominal diameter for E-500. As far as the pore size distributions are concerned, they seem to be short tail lognormals. According to the flux distributions, the corresponding means and standard deviations are slightly lower than the equivalent diameter of γ-globulin and are close to 60% of the nominal value for E-100 and near 20% for E-500.

On the other hand, it is worth remembering that these pore diameters have been evaluated as purely determined by simple sieving considerations. Thus, no adsorption of the protein molecules and volume hindrance effects have been considered inside the pores. If the central values of the distributions so obtained were to reproduce the nominal sizes, it should be necessary to assume coverage ratios, θ_d, which are greater than those measured by desorption experiments (compare with θ in Tables 3 and 4). This can be due to a less tightly linked adsorption which should play a role in operative conditions, although it is easily removable by pressure washing. This should agree with the low values of θ (<1) obtained. Nonetheless, probably both friction and equilibrium partitioning at the pore entrances should be significant; in fact, they can be interpreted as leading to reversible adsorption. Dynamic adsorptions such as those obtained here, i.e., approximately 1/3 (E-100) and 2 (E-500) adsorption layers, seem reasonable and should correspond, in terms of volume hindrance effects, to nonfriction movement for molecules passing not closer than 1/3 or 2 molecular gyration diameters. On the other hand, both θ and θ_d increase with pore size, in good agreement with results reported in the literature (39, 40).

Nevertheless, it is worth noting that the pore size distributions in Figs. 4 and 5 refer to the real functional behavior of E-100 and E-500 membranes when used to crossflow ultrafiltrate proteins because adsorption will always be present. This, once again, confirms the necessity of a deep study of pore size distributions and retentions in real laboratory situations to understand the operational characteristics of ultrafiltration steps in separation processes. In our case, for example, it can be concluded that both

membranes give very similar retentions, so E-500 should be preferable, given that it allows higher fluxes through the membrane. This difference in fluxes decreases when the molecular weight of the protein increases, as shown in Fig. 3.

ACKNOWLEDGMENTS

The authors thank the CICYT (Comision Interministerial de Ciencia y Tecnología) project MAT-0568 of the Spanish Program on Materials and the Junta de Castilla y León action VA37/93 for their financial assistance.

SYMBOLS

A	coefficient of the Graetz–Lévêque correlation (dimensionless)
A_a	total area occupied by proteins (m^2)
A_m	cross-section area of the membrane (m^2)
a	exponent in Eqs. (7), (9), and (11) (dimensionless)
B	constant of the logistical curve (m)
C	exponent of the logistical curve (dimensionless)
c_m	membrane concentration in contact with the high pressure interface (w/w)
c_p	permeate concentration (w/w)
c_0	feed concentration (w/w)
D	diffusion coefficient (m^2/s)
d	equivalent diameter of the protein molecule (m)
d_h	diameter of the hydraulic channel (m)
d_n	pore diameter for a new membrane (m)
d_p	pore diameter (m)
d_u	pore diameter for a used membrane (m)
f	molecular friction coefficient (kg/s)
$f(x)$	log normal distribution function of x (dimensionless)
f_{max}	maximum frequency for the distribution of x (dimensionless)
f_d	differential distribution function (dimensionless)
I	ionic strength (normality)
J_s	volume flux of the solute (m/s)
J_v	volume flux (m/s)
$J_{v,t}$	volume flux transmitted through the nonrejecting fraction of pores (m/s)
J_w	water volume flux (m/s)
$J_{w,r}$	water flux transmitted through the rejecting fraction of pores (m/s)
$J_{w,t}$	water flux transmitted through the nonrejecting fraction of pores (m/s)

K constant in Eq. (11) (m^{1+3a}/s)
K_m mass transfer coefficient (m/s)
K_n normalization constant in Eq. (17) (m^4)
K_0 constant in Eq. (5) (kg/m·s)
K_0' constant in Eq. (7) ($m^2 \cdot g^a/mol^a \cdot s$)
k Boltzmann constant (J/K)
L length of the hydraulic channel (m)
$L_{p,n}$ permeability for a new membrane (m/Pa·s)
$L_{p,u}$ permeability for a new membrane (m/Pa·s)
M_w molecular weight of the proteins (dalton)
N cumulative pore density (m^{-2})
N_T total pore density (m^{-2})
R true retention coefficient (dimensionless)
R_o observed or apparent retention coefficient (dimensionless)
r hydrodynamic radii of a sphere (m)
$\langle s^2 \rangle^{1/2}$ gyration radii (m)
$\langle s^2 \rangle_0^{1/2}$ unperturbed gyration radii (m)
T temperature (K)
V molecular volume (m^3)
v recirculation speed of the feed solution (m/s)
x number of segments of the molecule (dimensionless)

Greek Letters

δ thickness of the concentration polarization film layer (m)
α exponent of the Graetz–Lévêque correlation (dimensionless)
α_η expansion parameter (dimensionless)
λ ratio of the mean projected solute diameter and the specific area of the pores (dimensionless)
μ average diameter of the pore size distributions (m)
σ geometric standard deviation for the pore size distributions (m)
ξ frictional coefficient for each segment of the polymer chain (kg/s)
ϕ coefficient of the mass transfer coefficient $(m/s)^{1-\alpha}$
η viscosity (kg/m·s)
$\eta(c_m)$ solution viscosity at concentration c_m (kg/m·s)
$\eta(0)$ solvent viscosity (kg/m·s)
θ coverage ratio of adsorption (dimensionless)
θ_d dynamic coverage ratio of adsorption (dimensionless)

REFERENCES

1. M. C. Porter, "What, When and Why of Membranes MF, UF and RO," *AIChE Symp. Ser.*, *73*, 83 (1977).

2. M. Cheryan, *Ultrafiltration Handbook*, Technomic, Lancaster, UK, 1986.
3. W. S. W. Ho and K. K. Sirkar, *Membrane Handbook*, Van Nostrand Reinhold, New York, N.Y., 1992.
4. V. Gekas, G. Trägrdh, and B. Hallström, *Ultrafiltration Membranes Performance Fundamentals*, Swedish Foundation of Membrane Technology, Lund, Sweden, 1993.
5. V. L. Vilker, C. K. Colton, and K. A. Smith, "Concentration Polarization in Protein Ultrafiltration," *AIChE J.*, *27*, 632 (1981).
6. J. D. Andrade, in *Surface and Interfacial Aspects of Biomedical Polymers, Vol. 2* (J. D. Andrade, Ed.), Plenum, New York, N.Y., 1985.
7. A. A. Kozinsky and E. N. Lightfoot, "Protein Ultrafiltration: A General Example of Boundary Layer Filtration," *AIChE J.*, *18*, 1030 (1972).
8. A. G. Fane, C. J. D. Fell, and A. Suki, "The Effect of pH and Ionic Environment on the Ultrafiltration of Protein Solutions with Retentive Membranes," *J. Membr. Sci.*, *16*, 195 (1983).
9. G. Jonsson, P. Johansen, and W. Li, "Influence of Membrane Fouling on Ultrafiltration and Microfiltration Process," in *Proceedings: Engineering of Membrane Process*, Garmish-Partenkirchen, Germany, 1992.
10. W. R. Bowen and Q. Gan, "Properties of Microfiltration Membranes: Flux Loss during Constant Pressure Permeation of Bovine Serum Albumin," *Biotechnol. Bioeng.*, *38*, 688 (1991).
11. J. D. Ferry, "Ultrafilter Membranes and Ultrafiltration," *Chem. Res.*, *18*, 373 (1936).
12. J. C. Giddings, E. Kucera, C. P. Russell, and M. N. Myers, "Statistical Theory for the Equilibrium Distribution of Rigid Molecules in Inert Porous Networks. Exclusion Chromatography," *J. Phys. Chem.*, *72*, 4397 (1968).
13. E. A. Mason, R. P. Wendt, and E. H. Bresler, "Similarity Relations (Dimensional Analysis) for Membrane Transport," *J. Membr. Sci.*, *6*, 283 (1980).
14. J. L. Anderson, "Configurational Effect on the Reflection Coefficient for Rigid Solutes in Capillary Pores," *J. Theor. Biol.*, *90*, 405 (1981).
15. E. D. Glandt, "Noncircular Pores in Model Membranes: A Calculation of the Effect of the Pore Geometry on the Partition of a Solute," *J. Membr. Sci.*, *8*, 331 (1981).
16. L. Zeman and M. Wales, "Steric Rejection of Polymeric Solutes by Membranes with Uniform Pore Size Distributions," *Sep. Sci. Technol.*, *16*, 275 (1981).
17. K. W. Limbach, J. M. Nitsche, and J. Wei, "Partitioning of Nonspherical Molecules between Bulk Solution and Porous Solids," *AIChE J.*, *35*, 42 (1989).
18. K. D. Knierim, M. Waldman, and E. A. Mason, "Bonds on Solute Flux and Pore Size Distributions for Non-Sieving Membranes," *J. Membr. Sci.*, *17*, 173 (1984).
19. K. D. Knierim and E. A. Mason, "Heteroporous Sieving Membranes: Rigurous Bonds on Pore Size Distributions and Sieving Curves," *Ibid.*, *42*, 87 (1989).
20. J. K. Leypoldt, "Determining Pore Size Distributions of Ultrafiltration Membranes by Solute Sieving—Mathematical Limitations," *Ibid.*, *31*, 289 (1987).
21. P. Aimar, M. Meireles, and V. Sanchez, "A Contribution to the Translation of the Retention Curves into Pore Size Distributions for Sieving Membranes," *Ibid.*, *54*, 321 (1990).
22. O. H. Lowry, N. J. Rosebrough, A. L. Farr, and R. J. Randall, "Protein Measurement with the Folin Phenol Reagent," *J. Biol. Chem.*, *193*, 265 (1951).
23. J. G. Kirkwood, *Proteins*, Gordon and Breach, New York, N.Y., 1967.
24. D. Malamud and J. W. Drysdale, "Isoelectric Points of Proteins: A Table," *Anal. Biochem.*, *86*, 620 (1978).
25. P. Prádanos, J. I. Arribas, and A. Hernández, "Hydraulic Permeability, Mass Transfer and Retention of PEG's in Cross-Flow Ultrafiltration through a Symmetric Microporous Membrane," *Sep. Sci. Technol.*, *27*, 2121 (1992).

26. S-. T. Hwang and K. Kammermeyer, *Membranes in Separations*, Robert E. Krieger Publishing Co., Malabar, USA, 1984.
27. G. B. Van den Berg, I. G. Rácz, and C. A. Smolders, "Mass Transfer Coefficient in Cross-Flow Ultrafiltration," *J. Membr. Sci.*, *47*, 25 (1989).
28. R. J. Young and P. A. Lovell, *Introduction to Polymers*, Chapman and Hall, New York, N.Y., 1994.
29. M. E. Young, P. A. Carroad, and R. L. Bell, "Estimation of Diffusion Coefficients of Proteins," *Biotechnol. Bioeng.*, *22*, 947 (1980).
30. A. S. Michaels, "Analysis and Prediction of Sieving Curves for Ultrafiltration Membranes: A Universal Correlation?," *Sep. Sci. Technol.*, *15*, 1305 (1980).
31. M. S. Le and J. A. Howell, "Alternative Model for Ultrafiltration," *Chem. Eng. Res. Des.*, *62*, 373 (1984).
32. R. Nobrega, H. de Balmann, P. Aimar, and V. Sanchez, "Transfer of Dextran through Ultrafiltration Membranes: A Study of Rejection Data Analyzed by Gel Permeation Chromatography," *J. Membr. Sci.*, *45*, 17 (1989).
33. M. Bodzek and K. Konieczny, "The Influence of Molecular Mass of Poly(Vinyl Chloride) on the Structure and Transport Characteristics of Ultrafiltration Membranes," *Ibid.*, *61*, 131 (1991).
34. D. R. Lu, S. J. Lee, and K. Park, "Calculation of Solvation Interaction Energies for Protein Adsorption on Polymer Surfaces," *J. Biomater. Sci., Polym. Ed.*, *3*, 127 (1991).
35. S. Nakatsuka and A. S. Michaels, "Transport and Separation of Proteins by Ultrafiltration through Sorptive and Non-Sorptive Membranes," *J. Membr. Sci.*, *69*, 189 (1992).
36. M. N. Sarbolouki, "A General Diagram for Estimating Pore Size of Ultrafiltration and Reverse Osmosis Membranes," *Sep. Sci. Technol.*, *17*, 381 (1982).
37. P. Prádanos, J. I. Arribas, and A. Hernández, "Retention of Proteins in Cross-Flow UF through Asymmetric Inorganic Membranes," *AIChE J.*, *40*, 1901 (1994).
38. P. Prádanos and A. Hernández, "Cross-Flow of Proteins through Asymmetric Polysulfonic Membranes. I. Retention Curves and Pore Size Distributions," *Biotechnol. Bioeng.*, *47*, 617 (1995).
39. B. C. Robertson and A. L. Zydney, "Protein Adsorption in Asymmetric Ultrafiltration Membranes with Highly Constricted Pores," *J. Colloid Interface Sci.*, *134*, 563 (1990).
40. W. M. Clark, A. Bansal, M. Sontakke, and Y. H. Ma, "Protein Adsorption and Fouling in Ceramic Ultrafiltration Membranes," *J. Membr. Sci.*, *55*, 21 (1991).

Received by editor November 29, 1995